PNAS

Stealth predator comb jelly

Stealth predation and the predatory success of the invasive ctenophore *Mnemiopsis leidyi*

Sean P. Colin[a,1], John H. Costello[b], Lars J. Hansson[c], Josefin Titelman[d], and John O. Dabiri[e]

[a]Department of Marine Biology and Environmental Sciences, Roger Williams University, Bristol, RI 02809; [b]Biology Department, Providence College, Providence, RI 02918; [c]Department of Marine Ecology–Gothenburg, University of Gothenburg, SE-405 30 Gothenburg, Sweden; [d]Department of Biology, University of Oslo, N-0316 Oslo, Norway; and [e]Graduate Aeronautical Laboratories and Bioengineering, California Institute of Technology, Pasadena, CA 91125

In contrast to higher metazoans such as copepods and fish, ctenophores are a basal metazoan lineage possessing a relatively narrow set of sensory-motor capabilities. Yet lobate ctenophores can capture prey at rates comparable to sophisticated predatory copepods and fish, and they are capable of altering the composition of coastal planktonic communities. Here, we demonstrate that the predatory success of the lobate ctenophore *Mnemiopsis leidyi* lies in its use of cilia to generate a feeding current that continuously entrains large volumes of fluid, yet is virtually undetectable to its prey. This form of stealth predation enables *M. leidyi* to feed as a generalist predator capturing prey, including microplankton (approximately 50 μm), copepods (approximately 1 mm), and fish larvae (>3 mm). The efficacy and versatility of this stealth feeding mechanism has enabled *M. leidyi* to be notoriously destructive as a predator and successful as an invasive species.

feeding current | flow | predator | prey | biological invasions

The planktonic predator, *Mnemiopsis leidyi* (Fig. 1) is a cosmopolitan lobate ctenophore native to near-shore marine pelagic communities along the Atlantic coasts of North and South America. As a highly versatile predator, *M. leidyi* has become a notorious invader, first appearing in the Black Sea in the early 1980s (1), and shortly thereafter in the Sea of Azov (2), the Sea of Marmara, and the eastern Mediterranean (3). It is now widely distributed in the Caspian Sea (reported in 1999) and Adriatic Sea (reported in 2005) (4), and has most recently established itself in the Baltic Sea (reported in 2006) (5) and parts of the North Sea (6). Its arrival in each of these regions has led to decreased zooplankton abundances and diversity (7–10), often with trophic cascades that increase phytoplankton standing stocks (10, 11). Even in its endemic range, *M. leidyi* has experienced phenological changes caused by climate change that have decimated seasonal copepod populations and resulted in unprecedented decreases in zooplankton biodiversity (12). Few other planktonic predators have received such notoriety for their ability to alter pelagic ecosystems. In this study we quantified the flow field generated by *M. leidyi* to understand the mechanistic basis for this ctenophore's predatory success. We then applied these data to published hydrodynamic thresholds of typical copepod prey to predict the predation potential of *M. leidyi* and we compared this potential to that of other important zooplanktivores.

Feeding rates and predatory impact of zooplanktivores such as *M. leidyi* are determined by the rate at which predators encounter and retain prey. For most predators, including fish and copepods, predation is determined by the volume of water that the predator can search for prey items per unit time, i.e., the encounter rate kernel (E), calculated as $\pi D^2 v$, where D is the detection distance and v is the relative velocity of the predator to the prey (13). Consequently, effective detection can greatly enhance encounter probability, and thus predation. Sophisticated mechanisms such as vision (14) and mechanoreception (15, 16) allow for fishes and copepod predators, respectively, to detect and encounter prey. To successfully capture encountered prey, predators must also strike and retain prey before the prey can detect and elude the predator.

Therefore, the feeding rate (or clearance rate), F, is determined by both the rate that prey are encountered and the efficiency with which they are retained ($F = aE$, where a is the retention efficiency). To avoid predation, many zooplankton detect fluid disturbances made by approaching predators. Thus, for efficient foraging, a predator's behavior should be sufficiently "quiet" and the attack carefully timed to avoid triggering an escape reaction from the prey (15).

Ctenophores are basal metazoans that may be the earliest diverging extant multicellular animal lineage (17). Unlike fish and copepods, ctenophores do not use vision or other remote detection mechanisms to increase encounter rates with prey or rapid accelerations to attack prey. Instead, *M. leidyi* use cilia lining their auricles to generate a feeding current that entrains and transports prey between the oral lobes and past tentillae extending from the mouth (18) (Fig. 1). Despite some identified mechanoreceptive abilities (19), prey do not appear to be detected by the ctenophore until the prey have entered the region encompassed by the oral lobes (defined as the capture zone). Prey are captured only after contacting either the tentillae or the inner surface of the oral lobes (18, 19) (Fig. 1B). For *M. leidyi*, the encounter rate kernel ($E_{Mnemiopsis}$) is therefore determined as $A \cdot u$, where A is the area of the elliptical opening between the lobes and u is the feeding current velocity relative to the ctenophore. Consequently, the rate at which *M. leidyi* encounters prey will largely be determined by the ctenophore's size and rate of water entrainment.

In this study we quantify the fluid interactions of *M. leidyi* using 2D digital particle image velocimetry (DPIV). We show that *M. leidyi* creates a laminar feeding current that enables it to process large amounts of fluid without creating mechanical disturbances detectable by its prey. Thus, *M. leidyi* is able to encounter large water volumes, retain entrained prey with great efficiency, and use a diverse spectrum of prey types. The efficacy and versatility of this stealth strategy contribute to the ecological success of *M. leidyi* in endemic and invaded planktonic communities.

Results

M. leidyi uses cilia lining its auricles to create a uniform, laminar feeding current [Reynolds number <10 using the distance between lobe tips (gap width) as the length scale] that slowly entrains fluid between the oral lobes (Fig. 2). Fluid passing the lobe tips moves at velocities slower than 2.0 mm s⁻¹ (Fig. 2). The fluid then accelerates over the mouth ridge (Fig. 2), where it diverges to between (red A in Fig. 1) or just outside the auricles (red B in Fig. 1). Both trajectories lead the fluid past tentillae, which serve as capture
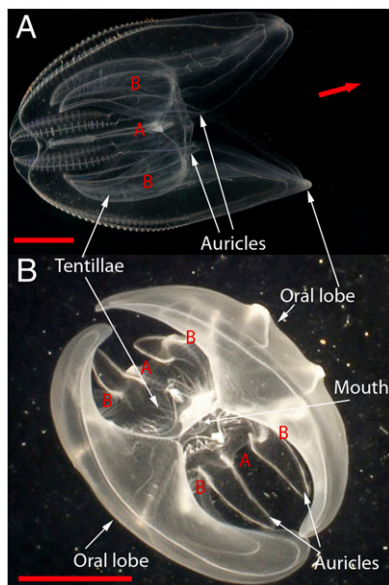
ECOLOGY

Fig. 1. (*A*) Side view of *M. leidyi* in foraging position with oral lobes open. The anterior and posterior ends are to the right and left, respectively. The oral lobes are capable of opening wider than shown. (*B*) Oral view showing important morphological features. Entrained fluid in the feeding current passes between the oral lobes and is diverted either between the adjacent auricles (red "A") or just outside the auricles (red "B"). Fluid encounters the tentillae with either trajectory. (Scale bars: 0.5 cm in *A* and *B*.) Red arrow in *A* indicates swimming direction.

surfaces and are covered with adhesive colloblasts. Fluid passing outside the auricles spirals in a corkscrew motion through an array of tentillae. As a result, *M. leidyi* can capture nearly 100% of the

prey that are transported past these tentillae (18) ($a \approx 100\%$). The volume of fluid entrained between the oral lobes over time (i.e., $E_{Mnemiopsis}$), representing a theoretical maximum clearance rate (F_{max}), increased as a square of total body length for hovering ctenophores (swimming velocity of 0; red circles in Fig. 3*A*). Swimming further increased the velocity of fluid passing through the oral lobes, such that $E_{Mnemiopsis}$ increased fourfold while *M. leidyi* were swimming (Fig. 3*B*). The theoretical F_{max} estimated from the entrained fluid was very similar to experimentally determined clearance rates of *M. leidyi* fed anchovy eggs and small zooplankton (Fig. 3*A*), implying near 100% retention efficiency.

Fluid deformation rates created by the feeding current remained low within *M. leidyi* prey capture regions between the oral lobes (Fig. 4). Fluid deformation was least near the lobe tips and in the central core of the volume between the lobes (Fig. 5). The highest deformation rates occurred along the inner surface of the oral lobes, as a result of boundary layer effects, and near the mouth (Fig. 5). In fact, deformation rates exceeded detection thresholds of typical copepods only in regions between the ctenophore lobes, i.e., within the capture zone. Mean and maximum deformation rates at the lobe tips increased slightly with swimming speed of the small ctenophore (2.0 cm) shown in Fig. 3*B* [Fig. S1 shows regression of deformation with swimming speed; mean deformation ($n = 15$), y = 0.01x + 0.09, $r^2 = 0.30$, $P = 0.04$; maximum deformation ($n = 15$), y = 0.09x + 0.24, $r^2 = 0.35$, $P = 0.03$) and decreased slightly for the medium ctenophore [4.1 cm; mean deformation ($n = 15$), y = −0.06x + 0.21, $r^2 = 0.51$, $P < 0.01$; maximum deformation ($n = 15$), y = −0.1x + 0.36, $r^2 = 0.69$, $P < 0.001$).

Discussion

Our estimates of F_{max} based on fluid flow measurements agree well with independent estimates of F based on feeding experiments (Fig. 3*A*), confirming the documented high capture effi-
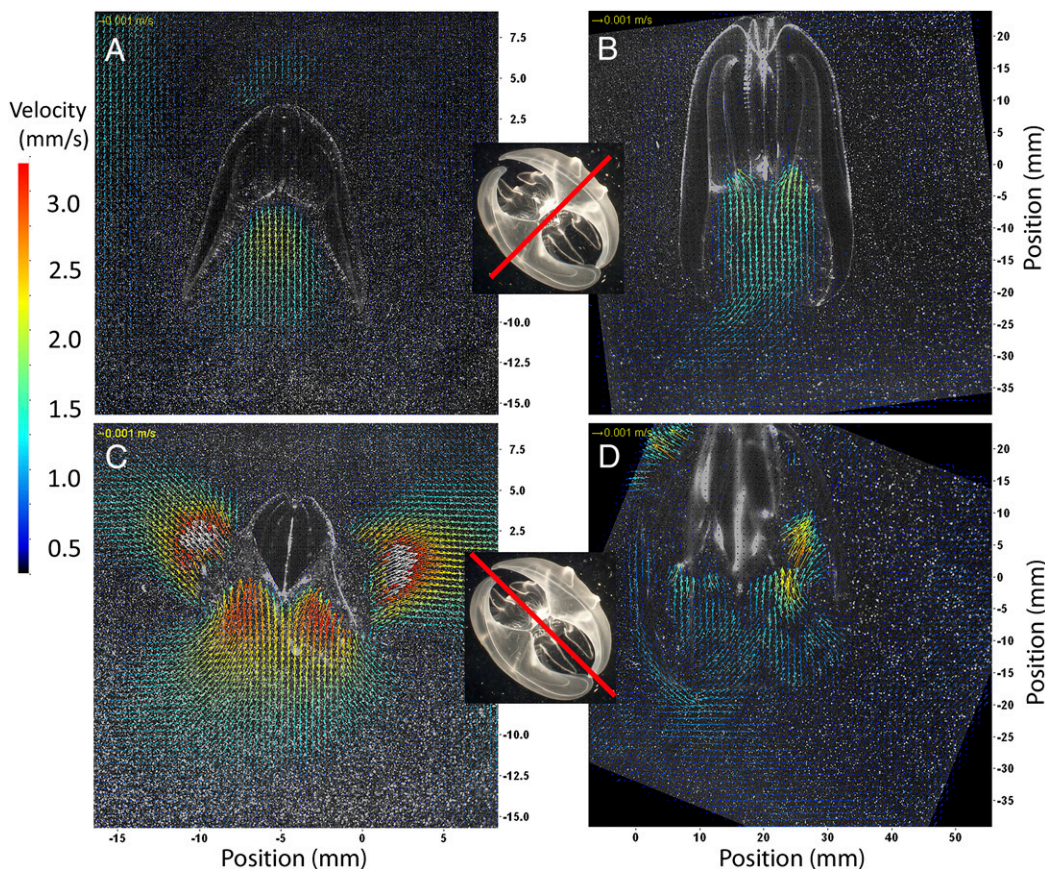

Fig. 2. Representative velocity vector fields around a small (1.3 cm long; *A* and *C*) and large (4.8 cm long; *B* and *D*) *M. leidyi*. Both ctenophores were stationary (i.e., swimming velocity of 0) and actively entrained fluid between their lobes. The laser sheet used for DPIV was directed through the center of the ctenophore at two perpendicular orientations (laser orientation illustrated by red line, *Insets*). DPIV is shown with the laser directed through the lobes (*A* and *B*) and between the lobes (*C* and *D*). This view is through the transparent lobe to show particle velocities between the lobes. White vectors represent velocities greater than 3.5 mm s⁻¹.
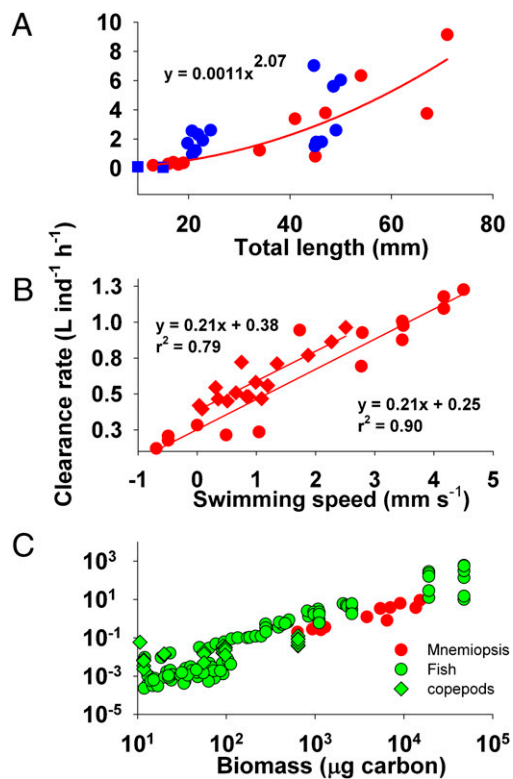
Fig. 3. (A) F_{max} based on volume flux between the lobes of *M. leidyi* ($E_{Mnemiopsis}$) as a function of ctenophore length (red symbols; swimming velocity of 0). The amount of fluid entrained over time increases with size to a power of approximately 2 and closely matches clearance rates from laboratory feeding experiments of *M. leidyi* fed anchovy eggs (40) (blue circles) and copepod nauplii and copepodites (41) (blue squares). (B) The amount of fluid that is entrained between the lobes increases linearly with increased swimming velocity of the ctenophore. Data are shown for two ctenophores (2.0 cm length, circles; 4.1 cm length, diamonds) swimming at different velocities. (C) Clearance rates of *Mnemiopsis* are on the same order of magnitude as those of zooplanktivorous fish and copepods (Table S1 shows sources of copepod and fish data).

ciency by *M. leidyi* on small prey ($a \approx 100\%$) (18). A comparison of carbon-specific clearance rates of fish and copepod predators demonstrates that feeding-current predation by hovering *M. leidyi* enables the ctenophore to feed at similar rates as predatory fish and copepods (Fig. 3C). This is probably a conservative estimate of predation potential because *M. leidyi* may more than double $E_{Mnemiopsis}$ by increasing swimming velocities, and hence, prey transport to capture surfaces (Fig. 3B).

For these high encounter volume rates to translate into high clearance rates, *M. leidyi* must capture most of the encountered prey. *M. leidyi* accomplishes this for small (40–200-μm length) prey with limited escape capacities, such as dinoflagellates, rotifers, and copepod nauplii, simply by directing entrained prey past highly efficient capture surfaces (18). However, in situ gut content data show that *M. leidyi* also effectively ingests larger copepods (approximately 1 mm in length) (20). The escape behavior of copepods relies on excellent detection of fluid deformation generated by approaching predators (21–23). Copepods also have some of the shortest reaction times (2 ms) (24) and they are capable of escaping at speeds greater than 800 body lengths s^{-1} (23). For successful capture of copepods, a large, slow-swimming predator such as *M. leidyi* must remain undetected until after the encounter with the prey. Other gelatinous predators accomplish this by foraging as "sit-and-wait" ambush predators (25, 26). However, the mechanics of ambush foraging constrain their F_{max} (25, 26), greatly limiting their ecological impact (26, 27).
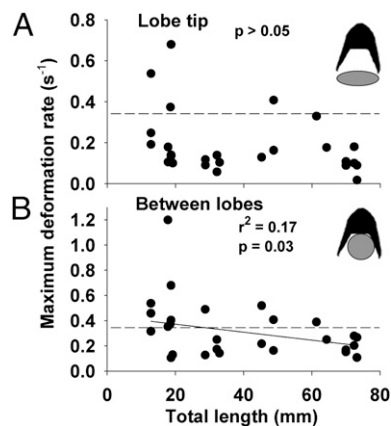

Fig. 4. Maximum observed fluid shear deformation rates (S_{yx}) at the region between or anterior to the lobe tip (*A*, *Top*) and the region between the lobes (*B*) of *M. leidyi* of various lengths ($n = 26$). The dashed line indicates the lowest reactive threshold of copepod prey (Fig. 5 shows threshold references). Gray ovals in the schematics illustrate different regions.

The low velocities characteristic of the feeding current of *M. leidyi* result in shear deformation rates that remain below the detection limits of their copepod prey (Fig. 5). In fact, the rates of deformation observed around *M. leidyi* are an order of magnitude lower than those in the feeding current of predatory copepods (22, 28, 29) and in the suction flow of fish (30). Low deformation rates enable ctenophores to transport copepods unwittingly into the capture zone between the oral lobes. In this region, *M. leidyi* is capable of detecting copepods and closing the lobe opening before the copepod reaches the high deformation regions (19). By closing the oral lobes around a copepod *M. leidyi* envelopes a package of water containing the copepod. At that point, the copepod may detect the high deformation rate and respond with one or more escape jumps. Most often the escape attempt fails and the trapped prey eventually becomes enmeshed upon the sticky inner surface of the lobe (19). As a result, *M. leidyi* captures most copepods ($a > 70\%$) that enter the region between the lobes (19). Most captures result from the copepod jumping into the inner lobe surfaces and only a small proportion of prey are captured on the tentillae surrounding the mouth (18). Although some sensory capabilities of *M. leidyi* have been recognized (19) and sensory cilia identified (31), it is still largely unknown how *M. leidyi* detects its prey. However, the feeding current that we have characterized is similarly laminar to that of filter feeding copepods, such as *Euchaeta* species (21), which have the ability to sense and locate, with relatively high precision, even small prey in their feeding current (21). Also, a laminar feeding current potentially may facilitate prey detection by *M. leidyi*.

Ciliary feeding currents are a common foraging strategy used by benthic suspension feeders such as bivalves, ascidians, and bryozoans, and are highly effective at processing large volumes of water. For example, oysters and ascidians pump 5 to 10 L h^{-1} g^{-1} dry weight (32, 33). However, these ciliary feeding currents generate much higher deformation rates (34, 35) and are primarily used for grazing on plankton incapable of swimming out of the feeding current, e.g., phytoplankton. In contrast, the strategy of *M. leidyi* to generate a hydrodynamically silent feeding current allows it to forage on motile prey as a stealth predator.

Few studies have examined the feeding currents of other lobate ctenophores (36, 37), and to our knowledge none has examined them quantitatively. However, behavioral evidence suggests that *Bolinopsis* spp., another cosmopolitan lobate ctenophore, forages similarly and also feed on mesozooplankton (38). Unlike *M. leidyi*, *Bolinopsis* spp. have not been implicated in devastating predatory effects on zooplankton biodiversity. The reasons for the different impacts of these lobate ctenophores are not clear. However, they
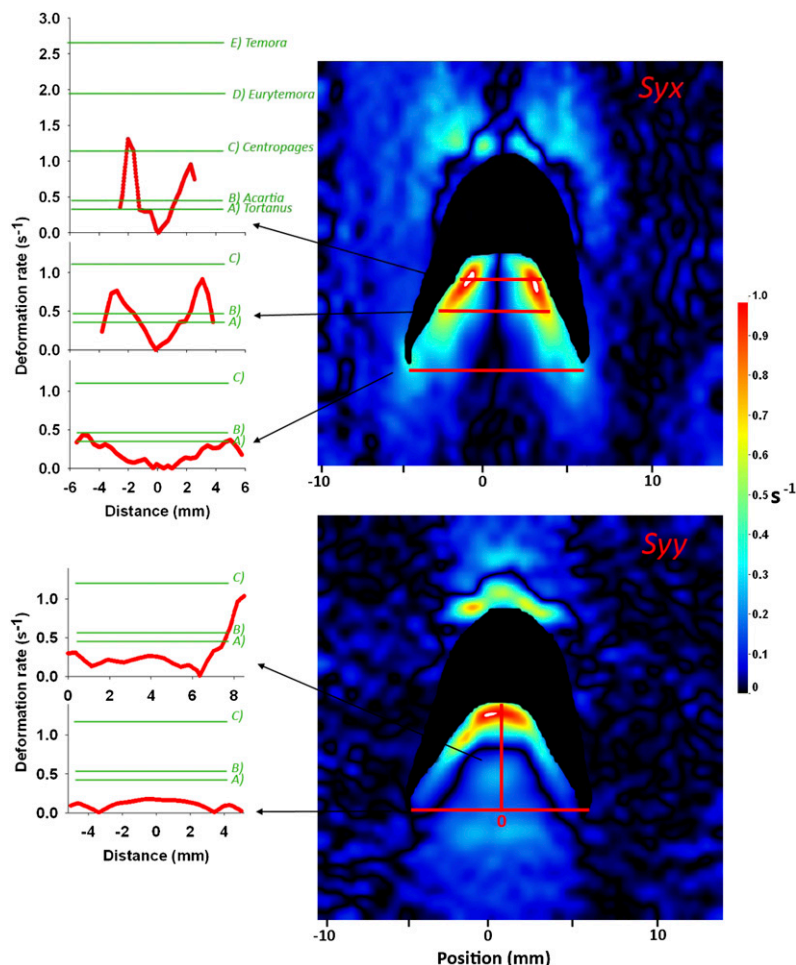
Fig. 5. Shear deformation rates of the two largest components of deformation in different regions of the feeding current of a small stationary *M. leidyi* (1.3 cm long). *Top*: S$_{yx}$ represents alterations in u_x (x component of fluid velocity) along the y axis. Three transects at outer, middle, and inner lobe positions (*Top, Right*) are compared with minimum threshold deformation rates that elicit escape responses of common coastal copepods (indicated by green lines with letters designating different copepod species). Deformation rate thresholds are from refs. 22 (*Acartia*), 42 (*Centropages, Temora, Tortanus*), and 34 (*Eurytemora*). *Bottom*: S$_{yy}$ represents alterations in u_y (y component of fluid velocity) along the y axis. Two transects depict S$_{yy}$ across the lobe opening and along a central axis from the lobe opening to the ctenophore's mouth (indicated by red lines, *Bottom*). Note that the observed deformation rates for this small ctenophore are large compared with those of larger ctenophores (Fig. 4). Despite this, much of the feeding current is undetectable to prey. We would expect a greater portion of the feeding current of larger ctenophores to be below the threshold of prey.

also differ in their life history strategies (38), metabolic demands (39), and physical tolerance. Each of these differences may contribute to the apparent ability of *M. leidyi* to better exploit coastal prey populations than does *Bolinopsis* spp.

The success of *M. leidyi* as an efficient stealth predator is based on its use of very basal structures—cilia—to move prey without those prey detecting the ctenophore's manipulation of the fluid. Because most zooplankton are guided by mechanical or chemosensory cues for predator detection, this foraging strategy provides access to a wide prey spectrum: both large and small zooplankters are vulnerable to predation by *M. leidyi*. The effective organization of these fundamental traits enables *M. leidyi* to function as both a versatile and efficient predator despite its phylogenetic and organizational simplicity.

Methods

Individual *Mnemiopsis leidyi* ctenophores were hand picked from docks adjacent to our laboratory at the Marine Biological Laboratories in Woods Hole, MA. They were immediately transported to the laboratory for examination. We estimated $E_{Mnemiopsis}$ for *M. leidyi* by quantifying the flow transported between its lobes. The quantified $E_{Mnemiopsis}$ equals the theoretical maximum volume clearance rate (i.e., $E_{Mnemiopsis} = F_{max}$ when $a = 100\%$). F_{max} is a useful metric because it can be compared with published clearance rates. The

flow transported between the lobes of *M. leidyi* was quantified using 2D DPIV. Individual ctenophores were placed into large glass filming vessels in filtered seawater seeded with 10-μm hollow glass beads. Ctenophores were then illuminated with a laser sheet (680-nm wavelength) at two orientations (i.e., two perpendicular cross sections; Fig. 2) and video recorded at 60 to 200 frames s^{-1} using a high-speed digital video camera (Fastcam 1024 PCI; Photron) placed perpendicular to the laser sheet. The velocities of particles illuminated in the laser sheet were determined from sequential images analyzed using a cross-correlation algorithm (LaVision Software). Image pairs were analyzed with shifting overlapping interrogation windows of decreasing size (64 × 64 pixels, then 32 × 32 pixels). This analysis generated velocity vector fields around the ctenophore (Fig. 2). $E_{Mnemiopsis}$ was estimated as the volume of fluid passing between the lobes as follows:

$$E_{Mnemiopsis} = Au = F_{\max} \qquad [1]$$

where u is the fluid velocity vectors entering the encounter zone integrated over the area, A, of the elliptical opening defined by the oral lobes. The area of elliptical opening ($A = \pi\alpha\beta$) was calculated using the oral lobe width and interlobe gap distance as the two axes of the ellipse ($\alpha = 1/2$ lobe width and $\beta = 1/2$ gap distance).

As copepods respond to spatial gradients in fluid velocities, we measured deformation in two perpendicular planes. This enabled us to measure the four components of 2D shear deformation (S$_{yy}$, S$_{yx}$, S$_{xx}$, S$_{xy}$) for two perpendicular cross-sections of *M. leidyi* generating a feeding current (Fig. 2 shows a diagram

and views of the cross-sections). Deformation rate components were calculated from measured planar velocity (u) fields as follows:

$$S_{yy} = \frac{du_y}{dy} \qquad \text{[2A]}$$

$$S_{yx} = \frac{du_x}{dy} \qquad \text{[2B]}$$

$$S_{xx} = \frac{du_x}{dx} \qquad \text{[2C]}$$

$$S_{xy} = \frac{du_y}{dx} \qquad \text{[2D]}$$

All ctenophores were oriented so that the y axis was always in the oral-aboral direction. Only two components of deformation (side view S_{yx} and S_{yy}) are shown in this study because they represent the maximum components observed among two views (side and lobe views) and the four components of 2D deformation (S_{yy}, S_{yx}, S_{xx}, S_{xy}) in each view. Consequently, these can be used to represent maximum strain rate (28, 29). A copepod will elicit an escape reaction when the deformation is greater than its threshold regardless of its direction (15, 22).

1. Vinogradov ME, Shushkina EA, Musaeva EI, Sorokin P (1989) New settler in the Black Sea—comb jelly *Mnemiopsis leidyi* (Agassiz). *Okeanologiya* 29:293–299.
2. Studenikina EI, Volovik SR, Mirzoyan ZA, Luts GI (1991) Comb jelly *Mnemiopsis leidyi* in the Azov Sea. *Okeanologiya* 31:722–725.
3. Shiganova TA, et al. (2001) Population development of the invader ctenophore *Mnemiopsis leidyi* in the Black Sea and in other seas of the Mediterranean basin. *Mar Biol* 139:431–445.
4. Shiganova TA, Malej A (2009) Native and non-native ctenophores in the Gulf of Trieste, Northern Adriatic Sea. *J Plankton Res* 31:61–71.
5. Javidpour J, Sommer U, Shiganova TA (2006) First record of *Mnemiopsis leidyi* A. Agassiz 1865 in the Baltic Sea. *Aquatic Invasions* 1:299–302.
6. Hansson HG (2006) Ctenophores of the Baltic and adjacent seas – the invader *Mnemiopsis* is here! *Aquatic Invasions* 1:295–298.
7. Kideys AE (2002) Ecology. Fall and rise of the Black Sea ecosystem. *Science* 297:1482–1484.
8. Oguz T, Fach B, Salihoglu B (2008) Invasion dynamics of the alien ctenophore *Mnemiopsis leidyi* and its impact on anchovy collapse in the Black Sea. *J Plankton Res* 30:1385–1397.
9. Roohi A, et al. (2008) Impact of a new invasive ctenophore (*Mnemiopsis leidyi*) on the zooplankton community of the Southern Caspian Sea. *Mar Ecol* 29:421–434.
10. Roohi A, et al. (2010) Changes in biodiversity of phytoplankton, zooplankton, fishes and macrobenthos in the southern Caspian Sea after the invasion of the ctenophore *Mnemiopsis leidyi*. *Biol Invasions* 12:2343–2361.
11. Kideys AE, Roohi A, Eker-Develi E, Mélin F, Beare D (2008) Increased chlorophyll levels in the southern Caspian Sea following an invasion of jellyfish. *Res Lett Ecol,* 1–5.
12. Costello JH, Sullivan BK, Gifford DJ (2006) A physical–biological interaction underlying variable phenological responses to climate change by coastal zooplankton. *J Plankton Res* 28:1099–1105.
13. Kiørboe T (2008) *A Mechanistic Approach to Plankton Ecology* (Princeton Univ Press, Princeton).
14. Hairston NG, Jr, Li KT, Easter SS, Jr (1982) Fish vision and the detection of planktonic prey. *Science* 218:1240–1242.
15. Kiørboe T, Visser A (1999) Predator and prey perception in copepods due to hydromechanical signals. *Mar Ecol Prog Ser* 179:81–95.
16. Fields DM, Yen J (2002) Fluid mechanosensory stimulation of behavior from a planktonic marine copepod, *Euchaeta rimana* Bradford. *J Plankton Res* 24:747–755.
17. Dunn CW, et al. (2008) Broad phylogenomic sampling improves resolution of the animal tree of life. *Nature* 452:745–749.
18. Waggett R, Costello JH (1999) Capture mechanisms used by the lobate ctenophore, *Mnemiopsis leidyi* preying on the copepod *Acartia tonsa*. *J Plankton Res* 21:2037–2052.
19. Costello JH, Loftus R, Waggett R (1999) Influence of prey detection on capture success for the ctenophore *Mnemiopsis leidyi* feeding upon adult *Acartia tonsa* and *Oithona colcarva* copepods. *Mar Ecol Prog Ser* 191:207–216.
20. Rapoza R, Novak D, Costello JH (2005) Life-stage dependent, in situ dietary patterns of the lobate ctenophore *Mnemiopsis leidyi* Agassiz 1865. *J Plankton Res* 27:951–956.
21. Fields DM, Yen J (1997) The escape behavior of marine copepods in response to a quantified fluid mechanical disturbance. *J Plankton Res* 19:1289–1304.
22. Kiørboe T, Saiz E, Visser A (1999) Hydrodynamic signal perception in the copepod *Acartia tonsa*. *Mar Ecol Prog Ser* 179:97–111.
23. Buskey EJ, Hartline DK (2003) High-speed video analysis of the escape responses of the copepod *Acartia tonsa* to shadows. *Biol Bull* 204:28–37.
24. Wagget RJ, Buskey EJ (2008) Escape reaction performance of myelinated and non-myelinated calanoid copepods. *J Exp Mar Biol Ecol* 361:111–118.
25. Hansson LJ, Kiørboe T (2006) Prey-specific encounter rates and handling efficiencies as causes of prey selectivity in ambush feeding hydromedusae. *Limnol Oceanogr* 51:1848–1858.
26. Regula C, Colin SP, Costello JH, Kordula H (2009) Mechanisms of prey selection in ambushing hydromedusae. *Mar Ecol Prog Ser* 374:135–144.
27. Hansson LJ, Moeslund O, Kiørboe T, Riisgaard HU (2005) Clearance rates of jellyfish and their potential predation impact on zooplankton and fish larvae in a neritic ecosystem (Limfjorden, Denmark). *Mar Ecol Prog Ser* 304:117–131.
28. van Duren LA, Stamhuis EJ, Videler JJ (2003) Copepod feeding currents: Flow patterns, filtration rates and energetics. *J Exp Biol* 206:255–267.
29. Catton KB, Webster DR, Brown J, Yen J (2007) Quantitative analysis of tethered and free-swimming copepodid flow fields. *J Exp Biol* 210:299–310.
30. Holzman R, Wainwright PC (2009) How to surprise a copepod: Strike kinematics reduce hydrodynamic disturbance and increase stealth of suction-feeding fish. *Limnol Oceanogr* 54:2201–2212.
31. Horridge GA (1965) Non-motile sensory cilia and neuromuscular junctions in a ctenophore independent effector organ. *Proc R Soc B* 162:333–350.
32. Fiala-Médioni A (1978) Filter-feeding ethology of benthic invertebrates (ascidians). IV. Pumping rate, filtration rate, filtration efficiency. *Mar Biol* 48:243–249.
33. Riisgård HU (1988) Efficiency of particle retention and filtration rate in 6 species of northeast American bivalves. *Mar Ecol Prog Ser* 45:217–223.
34. Green S, Visser AW, Titelman J, Kiørboe T (2003) Escape responses of copepod nauplii in the flow field of the blue mussel, *Mytilus edulis*. *Mar Biol* 142:727–733.
35. Maar M, Nielsen TG, Bolding K, Burchard H, Visser AW (2007) Grazing effects of blue mussel *Mytilus edulis* on the pelagic food web under different turbulence conditions. *Mar Ecol Prog Ser* 339:199–213.
36. Matsumoto GI (1991) Swimming movements of ctenophores, and the mechanics of propulsion by ctene rows. *Hydrobiologia* 216-217:319–325.
37. Matsumoto GI, Hamner WM (1998) Modes of water manipulation by the lobate ctenophore *Leucothea* sp. *Mar Biol* 97:551–558.
38. Falkenhaug T (1996) Distribution and seasonal patterns of ctenophores in Malangen, northern Norway. *Mar Ecol Prog Ser* 140:59–70.
39. Kremer P, Reeve MR, Syms MA (1986) The nutritional ecology of the ctenophore *Bolinopsis vitrea*: Comparisons with *Mnemiopsis mccradyi* from the same region. *J Plankton Res* 8:1197–1208.
40. Monteleone DM, Duguay LE (1988) Laboratory studies of predation by the ctenophore *Mnemiopsis leidyi* on the early stages in the life history of the bay anchovy, *Anchoa mitchilli*. *J Plankton Res* 10:359–372.
41. Finenko GA, et al. (2006) Invasive ctenophore *Mnemiopsis leidyi* in the Caspian Sea: Feeding, respiration, reproduction and predatory impact on the zooplankton community. *Mar Ecol Prog Ser* 314:171–185.
42. Burdick DS, Hartline DK, Lenz PH (2007) Escape strategies in co-occurring calanoid copepods. *Limnol Oceanogr* 52:2373–2385.

ECOLOGY